IOSR Journal of Mechanical and Civil Engineering (IOSR-JMCE)
e-ISSN: 2278-1684,p-ISSN: 2320-334X, Volume 18, Issue 4 Ser. I (Jul. – Aug. 2021), PP 19-32
www.iosrjournals.org

Numerical Investigation of Strengthening Alternatives for RC Members to Enhance Blast Resistance

Marco Fouad[1], Mohamed N. Fayed[1], Gehan A. Hamdy[2], Amr Abdelrahman[1]
[1]*Structural Engineering Department, Faculty of Engineering, Ain Shams University, Egypt*
[2] *Civil Engineering Department, Faculty of Engineering at Shoubra, Benha University, Egypt*

Abstract:
Background*: Terrorist bombing is currently regarded a threat to almost all countries around the world as it leads to loss of human lives, damage of structures and infra-structure in addition to serious negative impact on security and economy. Being the main carrying elements in skeleton structures, if columns are damaged or collapsed due to blast this may lead to partial or progressive collapse of the structure. It is therefore essential to direct research to improve the resistance of columns to blast so as to provide protection to the structure*.
Materials and Methods*: This paper presents numerical finite element study of RC columns with different strengthening system subjected to near-field explosion. Three-dimensional finite element models are made for RC columns protected by two strengthening systems: steel jacket and reinforced polyurethane bricks (RPB) with light steel wrapping which were previously tested experimentally under near-field blast load. Dynamic nonlinear analysis is performed using LS-DYNA program and the results are compared with experimental results regarding deflections and failure shapes. Additionally, a numerical study is conducted to investigate the effect of several variables such as concrete compressive strength, steel jacket thickness and density and stress-strain curve of RPB on the deflection values and failure patterns.*
Results*: The numerical modeling approach was efficient in predicting the deformation and failure of RC members subjected to blast whether unstrengthened or blast retrofitted. Blast resistance of RC columns was improved by using higher concrete compressive strength, steel jacket with grater thickness and RPB with higher density.*
Conclusion: *The steel jacket protective system is more efficient than the reinforced polyurethane brick with light steel jacket, as it improved the failure shape and decreased the deflections.*
Keywords*: Blast; Nearfield explosion; RC column; Numerical modeling; Finite elements; Dynamic nonlinear analysis; Blast protection; Steel jacket; Reinforced polyurethane bricks, LS-DYNA.*

Date of Submission: 28-06-2021 Date of Acceptance: 12-07-2021

I. Introduction

Presently, all nations are suffering from the threat of terrorists' attacks which are catastrophic to human life, buildings and infra-structures, as well as to the nation's security. Terrorist bombing usually targets crowded areas with high population to cause as much damage as possible [1]. Bombing is achieved using different conducts from vans, cars or luggage, etc., then explosion waves are produced that cause damage to structural elements and may lead to which cause a damage for structure or progressive collapse. Computational methods available in the structural analysis field are also used to estimate the response of the structure to such loads and predict the consequence of blast loads. Several computer software are capable of coupled analysis such as LS-DYNA[2], ANSYS [3] and ABAQUS [4].

Columns are the main structural element that support all floors and resist lateral loads (wind, seismic, blast load). Therefore, the columns play an important role in facing the blast loads and avoiding a sudden collapse of the structure. Hence, the columns should be capable of resisting the effects of explosion waves. Retrofitting of columns by different methods was studied by researches to enhance the columns resistance to blast loads. Strategies for blast protection to prevent collapse may be classified into the main categories as follows [5,6]: 1) creating a safe area by placing fences to avoid a near field explosion, 2) external strengthening of the columns to increase their ductility and strength, and 3) sacrificial cladding layers around the column to absorb blast energy.

Retrofitting of reinforced concrete (RC) columns with steel jacket is one of the most widely used retrofit techniques [7, 8]. It used made by wrapping the columns with steel sheets, steel strips or steel bars in the transverse direction to enhance the confinement of columns. The advantages of steel jacket retrofitting system are minimizing the construction time, increasing the column cross-sectional area, moderate cost and possible achievement of the architectural requirements instead of increasing the dimensions of columns [9]. The retrofitting

technique using steel jacket was shown to significantly improve blast performance of columns and their residual axial capacity after blast event; numerical results using ABAQUS software were compared with the experimental test for same different technique that leads to same deflection values and failure shape and it was concluded that using steel channel is more efficient than other models [10]. Another retrofitting system, classified above as the third strategy protection system, is by sacrificial cladding using reinforced polyurethane brick with light jacketing of steel #20 (0.89 mm of thickness)[11]. Polyurethane brick (foam) has a big variety of industrial with large range of densities to achieve the requirements and situations. It is a light-weight material, sound, fire resistant, low in thermal and energy absorbing. Using polyurethane brick was found to increase energy dissipation and decreases the deformation values[12]. The two retrofitting techniques are investigated numerically in this research.

Blast loads are waves of energy that are emitted as a result of a detonation which propagate in the atmosphere in radial shape. The dynamic pressure wave has a time history consisting of positive and negative phases. The explosion is classified to two pressure types: incident pressure (P_{so}) and reflected pressure (P_r), as shown in figure 1. The incident pressure is defined as massive pressure achieve a higher pressure than the ambient atmospheric pressure (P_o) [13].

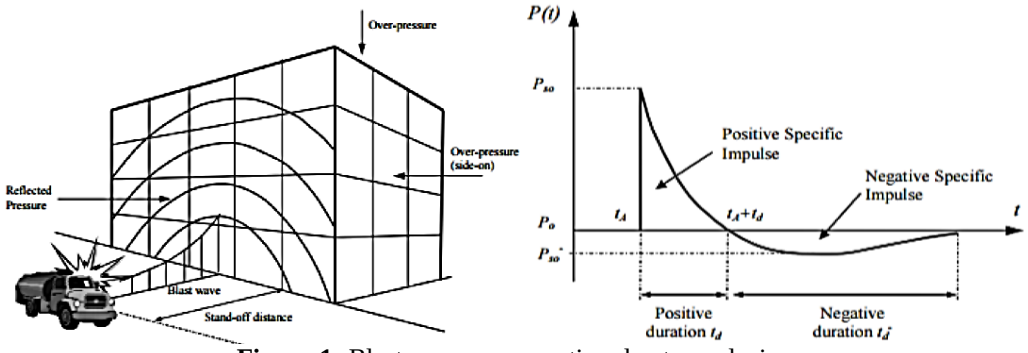

Figure 1: Blast waves propagation due to explosion

The explosive wave scaling value is identified by a scale equation with parameters related to pressure time history; the most common scaling relationship is the Hopkinson-Cranz or "cube-root" scaling, given by equation (1)[14].

$$Z = \frac{R}{W^{1/3}} \quad (1)$$

The characteristic pressure time history for blast load as shown in figure (1), the effect of a blast load can be classified to two durations: compression and suction pressure. The compression pressure happens when the incident pressure acting upon the building is more than the ambient atmospheric pressure. The time period is the time that the incident pressure is over the normal (ambient) pressure is referred to as the positive time duration (t_d^+) the area of the positive duration which clarified in figure 1 is defined as positive specific impulse *(I+)*. The negative (suction) pressure happens when the incident pressure acting upon the building is less than the ambient (normal) atmospheric pressure. The pressure time history for blast pressure can be defined using Friendlander relation in equation (2) [15].

$$P(t) = Ps_o \left(1-\frac{t}{t_d^+}\right) e^{\frac{-bt}{t_d^+}} \quad (2)$$

where *P(t)* is the pressure at time *t* is, *P* is the peak overpressure (reflected or incident), *b* is the waveform, and (t_d^+) is the positive phase duration of the blast pressure [16].

II. Numerical Modeling and Validation

The efficiency of blast retrofitting of RC columns is investigated numerically by creating three-dimensional finite element (FE) models for RC columns and carrying nonlinear dynamic analysis under near-field blast load using commercial computer software LS-DYNA. Two blast retrofitting techniques for RC columns are investigated: steel jackets with different parameters and polyurethane brick with light jacketing of steel. Validation of the modeling approach is made by comparing the numerical results to columns which have been experimentally tested under blast load in previously published research regarding the deflections and failure shapes.

Description of the Studied Column: The column specimen experimentally tested by Codina et al. [17], shown in figure 2, has a square section with dimensions 230mm x 230mm and length 2.44m. The ends of column member supports are fixed using a concrete block. The explosion material weight is 8 kg of TNT which charges at distance 0.32m near to one end of column and the standoff distance is 0.60m measured from member surface to

the center of the TNT charge, figure 2 shows the tested specimen and experimental test setup [17]. The reinforcement is made in directions: 12 longitudinal bars have diameter 8mm, in the transverse direction bars with diameter 6mm have spacing 60mm at the ends supports and 80mm at the middle length, as shown in figure 2(a). The maximum deflection is measured experimentally using LVDT and from FEA results at 1.52m from the end support.

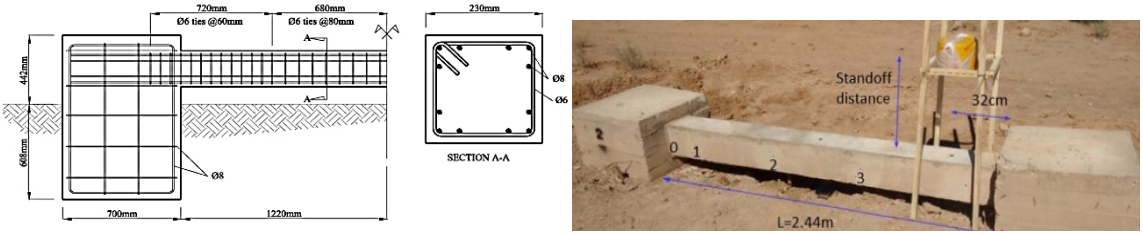

(a) (b)

Figure 2: Reinforced concrete member (a) concrete dimensions and reinforcement details, (b) test setup [17]

Numerical Modeling: LS-DYNA finite element software package is used to simulate the outcome of blast load on the structure elements; it has numerous materials identification and carries out nonlinear dynamic analysis utilizing combined different materials [18, 19]. The finite element model is created in the LS-Preprocessor and evaluated by LS-DYNA; the materials are defined as detailed in the next sections with respect to the behavior under explosion load. Figure 3 shows the 3-D finite element model of the validation model; the concrete column is modelled by eight-node solid elements with mesh size approximately 23 x20 mm and properties given in table 2. Steel longitudinal bars and stirrups are represented by beam element, with properties given in table 3.

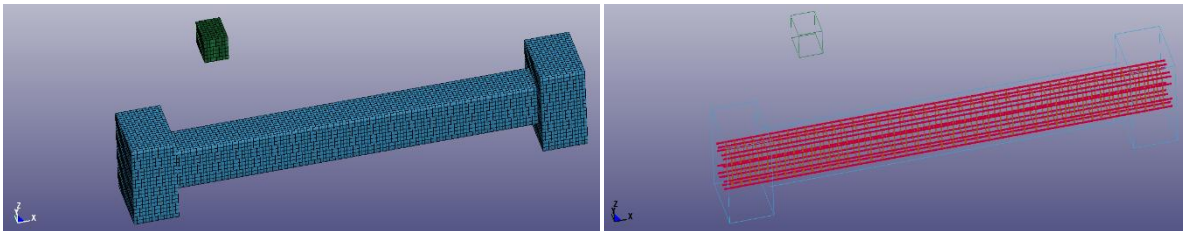

(a) Concrete column, explosive and air field (b) Main reinforcement bars and stirrups

Figure 3: Finite element model

Material Models:

Concrete material: The concrete material is modeled using MAT084 (MAT_WINFRITH_CONCRETE), the material model parameters given in table 3 represent the experimental work. Concrete is generated as continuum element model which is able to represent the complex compression and tension behavior as shown in figure 4 [20]. The model constraints include modulus of elasticity, compressive strength and reinforcement yield stress. The erosion value of concrete is 0.12, chosen to be a suitable value for the FE model to yield results compatible with the experimental results.

Steel material: The steel material is used to present the reinforcement bars (transverse and longitudinal reinforcement) that defined using material type (MAT 024: MAT_PIECEWISE_LINEAR_ PLASTICITY) [21]. Figure 4 illustrate the relationship between stress and strain of steel under ASTM strain rate and rapid strain rate due to dynamic load, the material model parameters used as shown in table 2 to be compatible with test setup.

Table 1: Concrete material parameters as per LS-DYNA package

Parameter	Value	Parameter	Value
Mass Density (R_0) (kg/m³)	2400	Fracture energy (FE)	65
Initial tangent modulus of concrete (TM)	2.641E+10	Aggregate size (ASIZE)	0.008
Poisson's ratio (PR)	0.20	Uniaxial tensile strength (UTS)	3000000
Uniaxial compressive strength (UCS)	3.00E+07		

Table 2: Steel material parameters adopted in LS-DYNA

Parameter	Value
Mass density (R_0) (kg/m³)	7850
Young's modulus (E)	2.05E+11
Poisson's ratio (PR)	0.30
Yield stress (SIGY)	4.20E+08

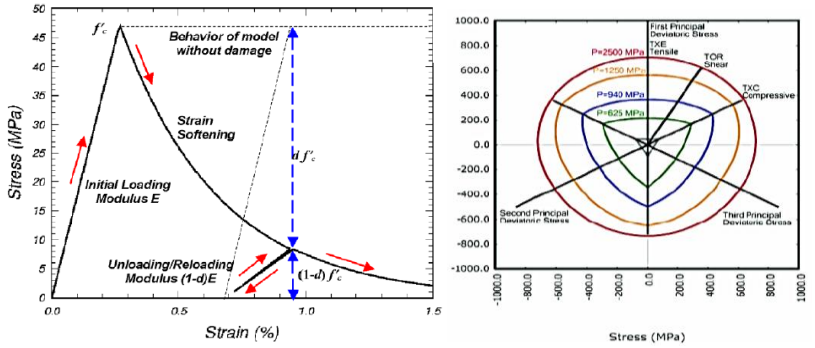

Figure 3: Properties of CSCM concrete material

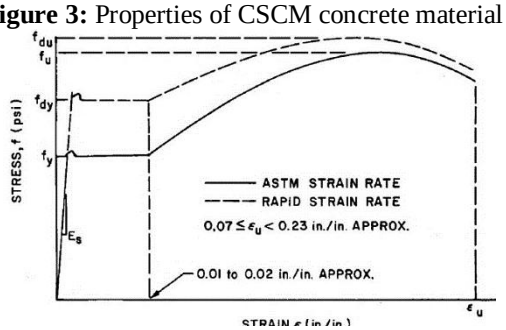

Figure 4: Stress-strain curve for steel material

Air modeling assumption: The air medium was used in case study that the blast wave propagated through air medium using ideal gas equation (3). Air was defined as material type (MAT_NULL_TITLE) [22] with the hourglass coefficient equals to $1x10^{-6}$ and the mass density is 1.29 kg/m³. Table 3 lists the values of air modeling parameters.

$$p = C_0 + C_1 \mu + C_2 \mu^2 + C_3 \mu^3 + E (C_4 + C_5 \mu + C_6 \mu) \quad (3)$$

For an ideal gas, this equation can be compacted by suitable coefficients:

$$(C_0 = C_1 = C_2 = C_3 = C_6 = 0,\ C_4 = C_5 = (\Upsilon - 1)$$

where $\mu = \frac{\rho}{\rho_0} - 1$ (4)

$$p = (\Upsilon - 1)\frac{\rho}{\rho_0} - 1 \quad (5)$$

where ρ_0 and ρ are the initial and actual densities of air, E specific energy and γ is the adiabatic expansion coefficient.

Table 3: Air modelling parameters adopted in the numerical model

Symbol	Description	Value
R_0	Mass Density	1.293 (kg/m^3)
C_0, C_1, C_2, C_3 and C_6	The polynomial equation coefficients	0
C_4 and C_5	The polynomial equation coefficients	0.40
E_0	Initial internal energy per unit volume	2.50x10^5(Pa)
V_0	Initial relative volume	1.00
Υ	The adiabatic expansion coefficient for air	1.40

Explosive material model: The blast load is modelled with 8-node finite elements using the material model (MAT_HIGH_EXPLOSIVE_BURN) with the knowledge (INITIAL_DETONATION) [23], the weight of blast load is defined in the FE model by using the volume and the density of explosive material. By using Jones-Wilkins-Lee (JWL) equation of state defines pressure as a function of relative volume, V, and internal energy per initial volume, E, C1, C2, r1 and r2 are constants and e, ω and v are the internal energy, γ adiabatic constant and specific volume respectively, and its standards for explosives restricted by dynamic tests as per equation (6) [24].

$$P = C_1 \left(1 - \frac{\omega}{r_1 V}\right) e^{-r_1 v} + C_2 \left(1 - \frac{\omega}{r_2 V}\right) e^{-r_2 v} + \frac{\omega e}{v} \quad (6)$$

Table 4 presents the TNT material modelling parameters according to the experimental data such as the type of explosive material and its weight, also it clarified the other parameters related to the velocity, volume, energy and mass density [25].

Table 6: Modeling parameters for explosive material

Parameter	Value	Parameter	Value
Mass density (R_0) (kg/m³)	1600	R1 (Parameter)	5.10
Detonation velocity (D) (m/s)	7680	R2 (Parameter)	1.50
C-J pressure (PCJ) (Pa)	$2.11x10^{10}$	OMEGA (Parameter)	0.29
A (parameter, C1) (Pa)	$7.59x10^{11}$	E_o (Initial internal energy per unit volume (Pa)	$4.50x10^{10}$
B (parameter, C1) (Pa)	$1.256x10^{10}$	V_o (Initial relative volume)	1.0

Numerical results and comparison with experimental results: Figure 5 shows the experimental and numerical failure shapes and pressure-time history for RC element under of 1.0 kg equivalent TNT explosion. The numerical failure shape is close to the experimental failure shape showing splitting of the concrete cover and deflection of the structural element. The maximum deflection measured experimentally and computed by finite element model were 67.20mm and 66.50 mm, respectively, with difference 1.04%. Comparison between the pressure-time history graph of the experimental and FE model in Figure 5 (c) shows that the overpressure is close to each other.

(a) Experimental failure shape [17]

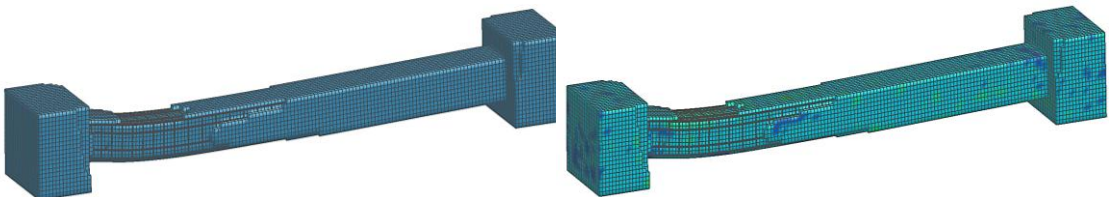

(b) FE model failure shape

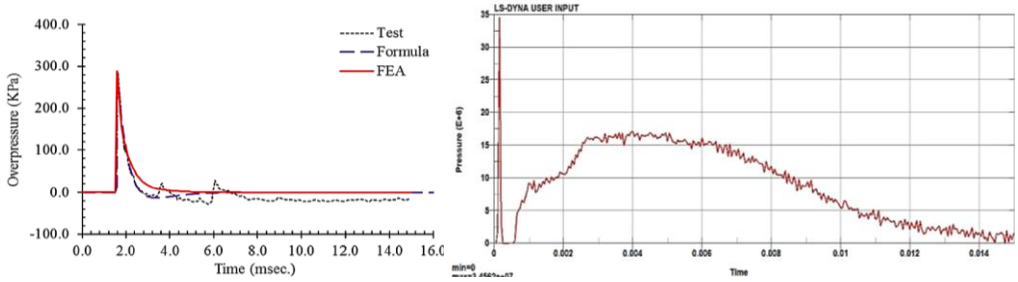

(c) Pressure effect and experimental and FE model overpressure values.

Figure 5: Comparison between FE model and experimental failure shapes and overpressure values

III. Near-Field Explosion Effect on Blast Retrofitted Members

Blast Retrofit Using Steel Jacket System:

The steel jacket proved to be a highly efficient retrofitting system for resisting blast load due to it is efficiency to increase the ductility, strain ductility and enhance the lateral deformation[26]. Steel jacket is used to protect the RC member to improve the resisting of blast load by enhance the failure shape of RC element and the deflection values.

Experimental study case: In an experimental work by Codina et al.[12] wrapping steel plates around the RC element from four side and connecting at the front side with bolts to improve the contact between steel jacket and RC element, a shear keys with section UPN100 were welded at the ends of the RC element specimen to avoid any shear failure action. As validation for the numerical modeling approach, 3 D FE model was created for the RC member of this experimental study having the same concrete dimensions, steel reinforcement value, TNT weight, location of explosive material and material properties as shown in figure 6. The steel jacket consist of one layer of steel sheet with thickness of 3.25mm for each side. To investigate numerically the effectiveness of the steel jacket, 3D FE models were made using three different steel jacket thicknesses: 2.00 mm, 3.25mm and 5mm.

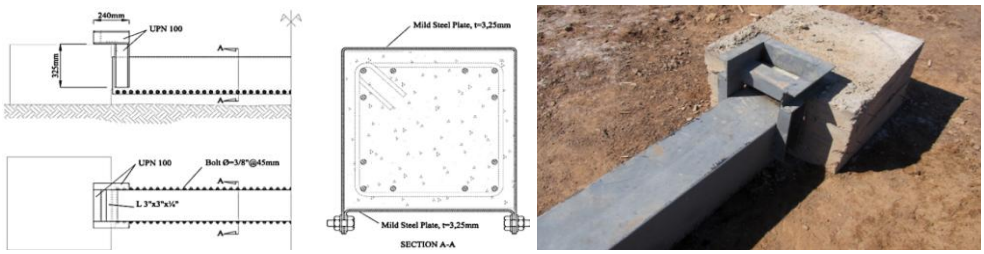

(a) (b)

Figure 6: RC member retrofitted with steel jacket (a) concrete and steel jacket dimensions, (b) test setup[12]

Numerical modeling: The steel jacket is modeled using 4-node shell elements using material (MAT_PLASTIC_KINEMATIC); this material is suited to isotropic model and kinematic hardening plasticity. The command (CONTACT_TIEBREAK_SURFACE_TO_SURFACE) is used to create the contact between the steel jacket and RC member. The RC member is defined as master surface, while the steel jacket is defined as the slave surface. The tie break contact allows the separation of the tied surfaces under tensile and shear loads using the strength-based failure, and has been proved efficient according to previous works [27, 28, 29].
Tiebreak contact allows the separation of the tied surfaces under tensile and shear loads using the strength-based failure

$$\left(\frac{|\sigma_n|}{NFLS}\right)^2+\left(\frac{|\sigma_s|}{SFLS}\right)^2 \geq 1 \quad (7)$$

Where, $\boldsymbol{\sigma_n}$: the normal stress, $\boldsymbol{\sigma_s}$: the shear stress, ***NFLS***: tensile failure stress and ***SFLS***: shear failure stress
Equation (7) was defined by Lu et al. [29] to approximate ***NFLS*** and ***SFLS*** values and was validate by Lu et al. [30]

$$NFLS=0.395f_{cu}^{0.55} =0.447\ (f_c')^{0.55} \quad (8)$$

Where $\boldsymbol{f_{cu}}$: the concrete cube compressive strength (MPa) and $\boldsymbol{f'_c}$: the concrete cylinder strength (MPa)

$$SFLS=1.5\beta_w\ NFLS \quad (9)$$

Where, $\boldsymbol{\beta_w}$: steel plate to RC concrete width ratio factor, which affects the bond-slip parameters, and is calculated by

$$\beta_w = \sqrt{\frac{2.25-b_f/b_c}{1.25+b_f/b_c}} \quad (10)$$

Where $\boldsymbol{b_c}$: the width of the RC member and $\boldsymbol{b_f}$: the width of the steel jacket
Numerical results and comparison with experimental results: Figure 7 shows the numerical results of failure shape and pressure for steel jacket retrofitted RC element as well as the experimental failure shape. The deformed shape of the steel jacket for experimental specimen is observed to be compatible with the FE deformed, there is an enlargement of steel jacket due to blast load which causes transverse deformation in both experimental and FE model. The pressure contour of the concrete element at time 1.486e+07 sec., shown in figure 7(b) indicates concentrated stresses at the top zone which is facing the overpressure according to the explosive material located. Therefore, the RC element starts to collapse from the top surface. The maximum deflection for steel jacket 3.25 mm recorded experimentally and computed numerically were 28.60 mm and 29.10 mm, respectively, with difference equal to 1.70%.

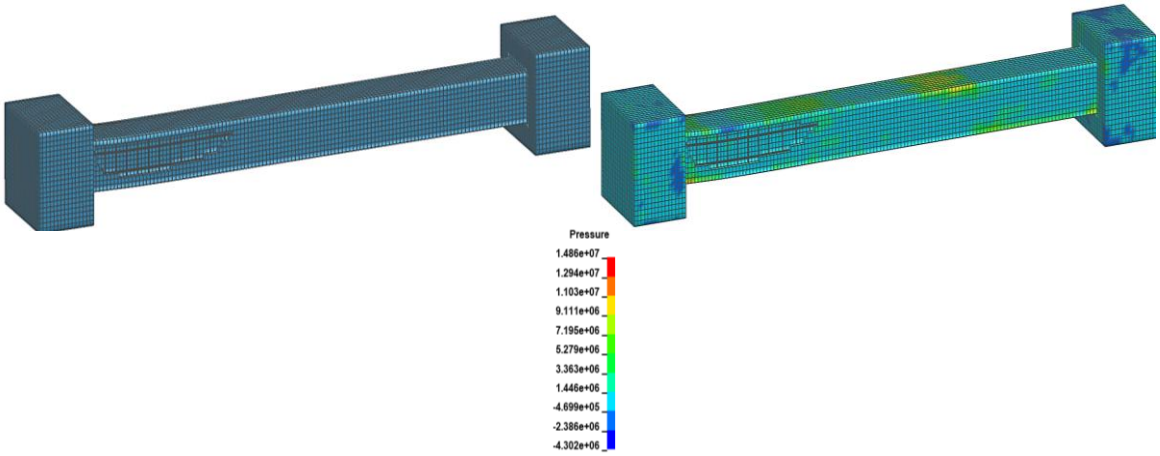

(a) FE model failure shape (b) Pressure effect

(c) Experimental failure shape [12]

Figure 7: Results for RC member retrofitted with steel jacket under blast

Blast Retrofit Using Reinforced Polyurethane Brick with Light Jacket:

Polyurethane brick is a crushable foam material suitable for resisting the shockwaves and impact absorption by dissipating energy [31]. It has many advantages such as low cost, compound compression performance and high efficiency of energy absorption [32]. Experimental study has been conducted to study the ability of foam to protect the structural element against the explosions and it was demonstrated as an operative and effectual sacrificial cladding due to its outstanding energy absorption capacity [33]. There are different types of foams material designed to crush under impact loads such as metallic, non-metallic foams and honeycombs, all of them are using to absorb energy and decrease the transfer of loads to the structure element behind them. The main material properties for foams can be defined by compressive stress-stain curves, described by initial elastic region tracked by a plateau stress of foam equation representing plastic yielding, as shown in figure 8 [34, 35].

The plateau stress of the foam is described by the equation

$$\frac{\sigma_{pl}}{\sigma_{ys}} \approx 0.30\ (\varphi\frac{\rho_f}{\rho_s})^{3/2} + (1-\varphi)\ \frac{\rho_f}{\rho_s} + \frac{p_0 - P_{atm}}{\sigma_{ys}} \qquad (11)$$

Where σ_{pl} : is the plateau stress of the foam, σ_{ys}: is the yield strength of the parent material, φ: is the fraction of solid in the cell edges of the foam, ρf: is the density of the foam, ρs: is the density of the parent material, p_o :is the internal cell gas pressure, *Patm* is atmospheric pressure.

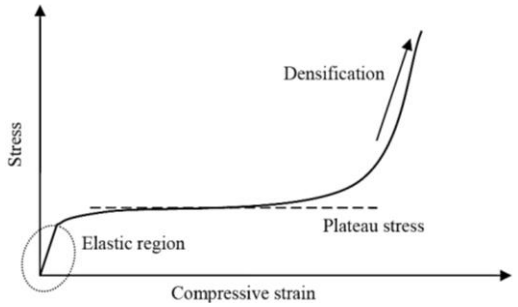

Figure 8. Typical stress-strain curve for crushable energy absorbing material

Different materials may be classified as crushable material which behave as energy dissipation material such as skydex convoy decking, Nomex honeycomb, alporas aluminum foam and expanded polystyrene (EPS), shown in figure 9. Figure 10 illustrates the deformation shape for the four types which give indication for the strength and response of each material for resist the shock waves, these profile shapes are measured across the plate centers between middle points of two opposite edges; the experimental results shows that the aluminum foam provided superior performance to other tested materials.

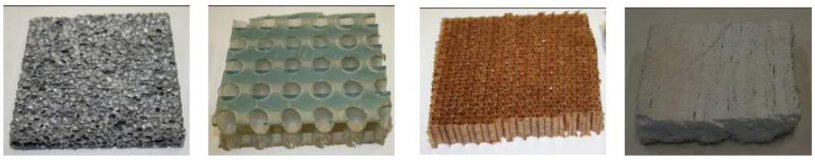

(a) (b) (c) (d)

Figure 9. Types of crushable materials: (a) Aluminum foam, (b) Skydex, (c) Nomex honey comb, and (d) Expanded Polystyrene (EPS)

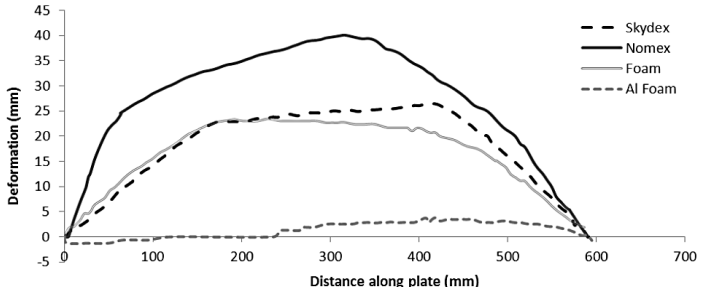

Figure 10. Stress-strain curve for different types of foam, crushable energy absorbing material deformation profile for materials, and plateau stress of the foam equation.

Experimental study case: Published research by Codina et al. [12], investigated experimentally the behavior of RC members protected by reinforced polyurethane bricks (RPB) type, one of foaming material which is used as a second approach as sacrificial cladding layers. The dimensions of the brick units are 230 mm x 240 mm x 145 mm and light steel jacket with thickness 0.89mm. Reinforcement bars with diameter 6 mm are embedded in the polyurethane blocks. Reinforcement bars are located to connect seven layers of galvanized steel and #14 mild steel bar. A light steel jacket with thickness 0.89mm is wrapped around the RPB and RC element, as shown in figure 11 [12].

(a) Reinforcement of polyurethane bricks (b) Placing RPB on test specimen

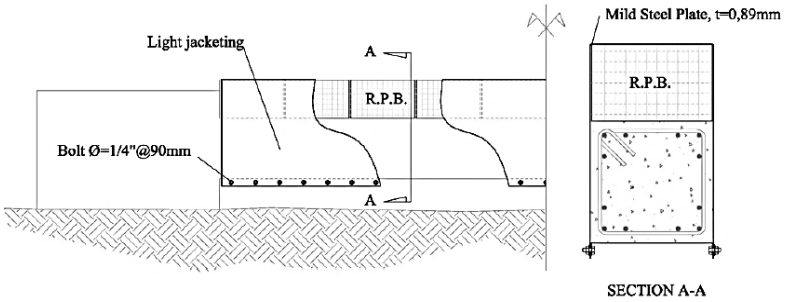

(c) Wrapping of RPB and RC section with light steel jacket

Figure 11. Test setup for retrofitting alternative using reinforced polyurethane brick with light steel jacket [12]

Numerical modeling: Finite element model was made for the experimental specimen using LS-DYNA software having the same data (materials, blast load, concrete dimensions and steel reinforcement for column). The foam material is represented in LS-DYNA using material MAT126 (MAT_MODIFIED_HONEYCOMB) which has been previous used by researchers [36, 37, 38] to model the anisotropic behavior for material properties of foam honeycomb crushable foams. Material MAT126 is a development of material MAT 026; however, some additional parameters are available as optional use [2]. Material MAT 126 defines three different yield surfaces: first, nonlinear elastoplastic material behavior is defined for all shear and normal stresses; secondly, a yield surface is distinct as the effects of off-axis loading; thirdly, second yield surface is identified by the sign of the first load curve ID. Table 7 lists the material properties of polyurethane bricks with light steel jacket used as sacrificial cladding for column retrofit.

Table 7 Material properties of polyurethane bricks as adopted in the numerical model.

Symbol	Parameter	Value
R_0	Density (kg/m^3)	569.30
E	Young's modulus for honeycomb material (MPa)	71000
PR	Poisson's ratio for compacted honeycomb material	0.19
SIGY	Yield stress for fully compacted honeycomb (MPa)	322
LCA, LCB, LCC	Load curve ID: yield stress as a function of the angle off the material axis in degrees.	Refer to figure (8)
LCS, LCAB, LCBC, LCCA	Load curve ID: damage curve giving shear ab-stress multiplier as function.	Refer to figure (8)
EAAU, EBBU, ECCU	Elastic modulus in uncompressed configuration (GPa)	500
GABU, GBCU, GCAU	Shear modulus G_{abu}, G_{bcu}, G_{cau} in uncompressed configuration (GPa)	920
TSEF	Tensile strain at element failure	0.045
SSEF	Shear strain at element failure	0.045

Numerical results and comparison with experimental results: Figure 12 shows the deformed shape and concrete splitting of the RC member retrofitted with RPB with 0.89mm light steel jacket and the FE results of pressure. It is observed that the failure shape is close to the experimental shape. The maximum deflections recorded experimentally and computed numerically are 52.50 mm and 52.70 mm, respectively, with difference of only 0.38%.

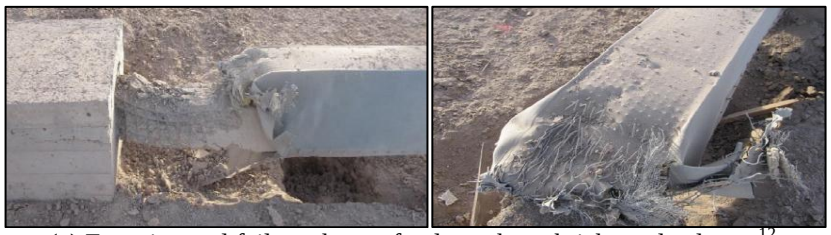

(a) Experimental failure shape of polyurethane bricks and column [12]

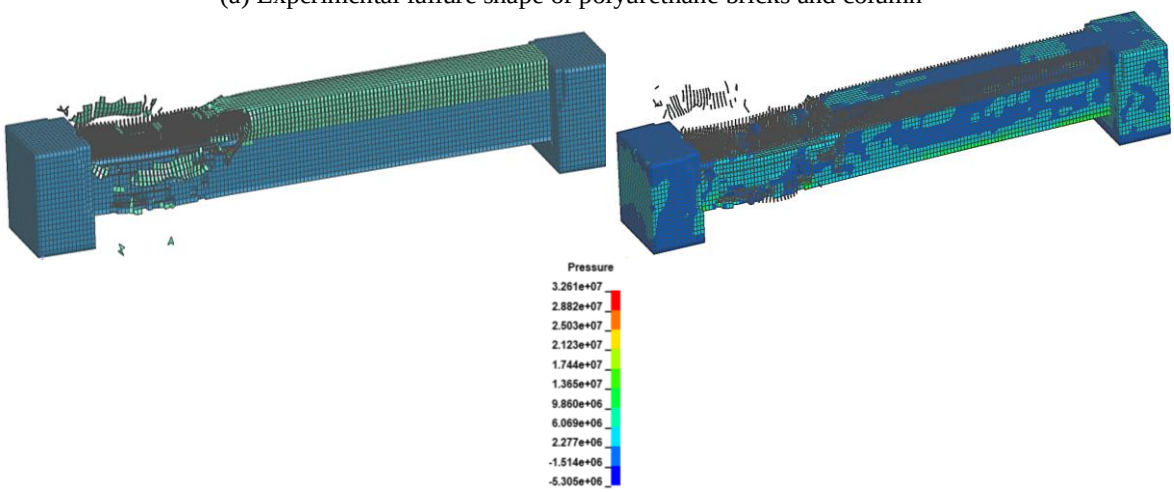

(b) FE model failure shape (c) Pressure effect

Figure 12: Experimental and numerical results for RC member retrofitted with PRB with light jacket under blast

IV. Numerical Study

Numerical study was made to investigate the effect of several parameters on the behavior of retrofitted RC columns under near-field explosions. Numerical modeling and nonlinear dynamic analysis were made using LS-DYNA software package following the previously explained procedure. The numerical results are presented and discussed in the following sections.

Effect of Concrete Compressive Strength: To investigate the effect of the compressive concrete strength on the deformation shape and the deflection values of RC member under blast load, FE models are made for the column with concrete compressive strength values of 40 MPa and 50MPa under blast load using the same explosive weight 8kg TNT and the same column dimension, reinforcement values and supporting system as in the previous study. The concrete material parameters adopted are listed in table 8. Numerical results show that

the maximum deflection values for the RC column with concrete compressive strength 30, 40 and 50 MPa were 66.50, 52.00 and 48.70 mm, respectively, indicating improvement of blast resistance for concrete with higher compressive strength. Also, higher compressive strength of concrete improved the failure mode through decreasing the distortion and splitting of concrete.

Table 8: Concrete material parameters adopted in the FE model

Parameter	Value	Parameter		Value
Mass Density (R_O) (kg/m³)	2400	Uniaxial compressive strength (UCS)	for fcu 30MPa	3.00E+07
Initial tangent modulus of concrete (TM)	3.055E+10		for fcu 40MPa	4.00E+07
Poisson's ratio (PR)	0.20		for fcu 50MPa	5.00E+07
Fracture energy (FE)	65	Uniaxial tensile strength (UTS)	for fcu 30MPa	3000000
Aggregate size (ASIZE)	0.008		for fcu 40MPa	4000000
			for fcu 50MPa	5000000

Effect of Thickness of Steel Jacket: FE models are made for RC columns with steel jacket of thickness 2.0 mm and 5.0 mm, in addition to the previous model for steel jacket thickness 3.25mm as in the experimental work. Figure 13 shows the numerically obtained failure shape for the columns retrofitted using three thicknesses of steel jacket when subjected to the same near-field explosion load. The deflection values for steel jacket thickness 2.00mm, 3.25mm and 5.00mm are 38.70mm, 29.10 mm and 21.80 mm, respectively. Decreasing the steel jacket thickness to 2.00mm, the member failure (concrete splitting, deformation) increased than experimental results using steel jacket 3.25mm.

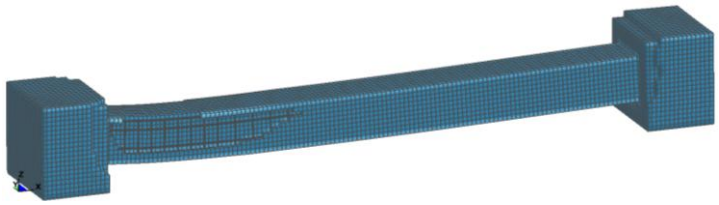

(a) RC element retrofitted with steel jacket thickness =2.00mm

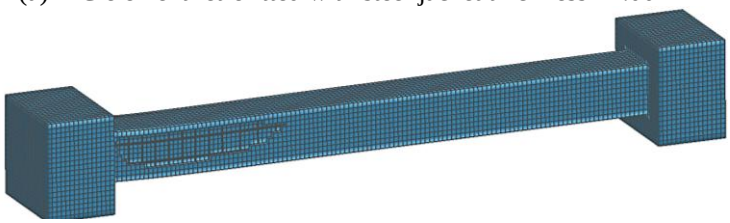

(b) RC element retrofitted with steel jacket thickness =3.25mm

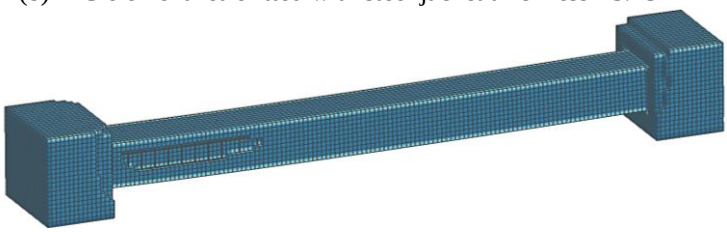

(c) RC element retrofitted with steel jacket thickness =5.00mm

Figure 13. Deformed shape of RC members retrofitted with steel jackets of different thicknesses under blast load

Effect of Density of Reinforced Polyurethane Brick Retrofitting System

A numerical study is carried out with different densities and stress-strain curves for the RPB system used as protective cladding system; the effect on the deformation shape and the deflection values is studied and compared.

Figure 14 shows the failure shape for the different studied densities.

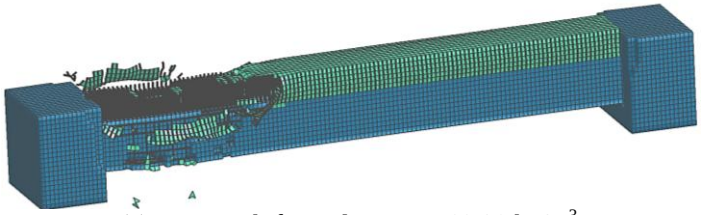

(a) RPB with foam density =569.30 kg/m^3

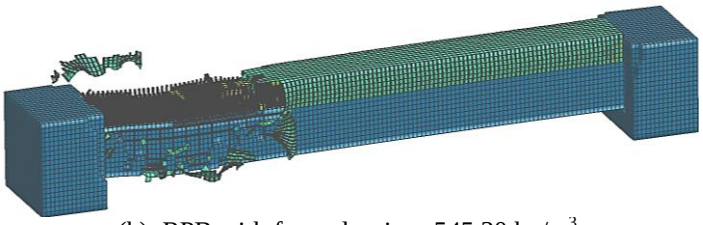

(b) RPB with foam density =545.30 kg/m^3

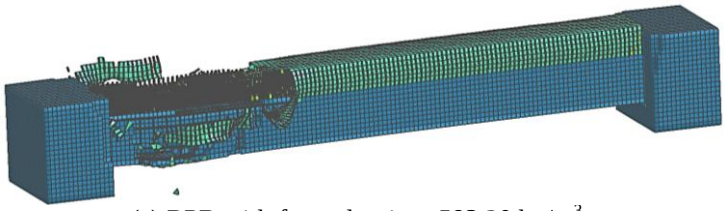

(c) RPB with foam density =593.20 kg/m^3

Figure 14. Failure shape of RC members retrofitted with RPB with different foam densities under blast load

V. Discussion

Three strategies of retrofitting systems of RC column against blast load: no blast retrofit, steel jacket, reinforced polyurethane brick with light steel jacket, are studied for the same column dimensions (230mmx230mm) and reinforcement (longitudinal bars 12T8 and transverse as seismically detailed). For all alternatives, the explosive charge weight is used 8 kg, the standoff distance measured from top surface of column is 60cm and 32cm from the support concrete block. The experimental and numerical results showed that the steel jacket protection system is the most efficient system and presented the best results for blast protection. Table 9 presents the deflection before failure for the three strategies; it is clear that the steel jacket yields better results than increasing concrete compressive strength and reinforced polyurethane brick. Moreover, the maximum displacement value of steel jacket is less than the two other strategies as shown in table 9. Figure 15 shows the difference between the three strategies of protecting column by using protective cladding or increase the concrete compressive strength, it is clear that the steel jacket outperform the two other strategies which decrease the deflection value by 60% comparing with the non-retrofitted alternative, and also, it is less than the reinforced polyurethane brick by 45%.

.

Table 9: Maximum lateral deflection for the retrofit alternatives

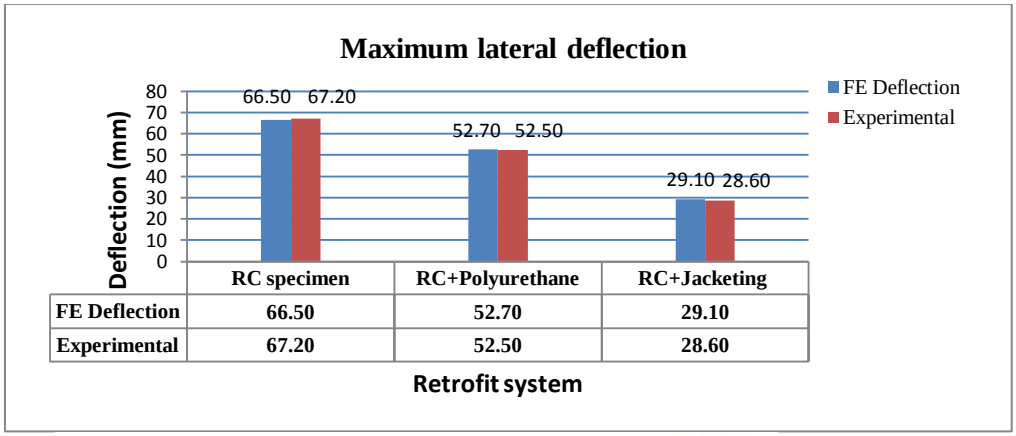

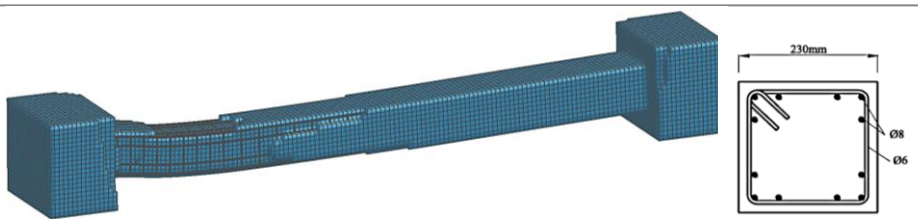

(a) Reinforced concrete column without retrofitting system (fcu=30MPa)

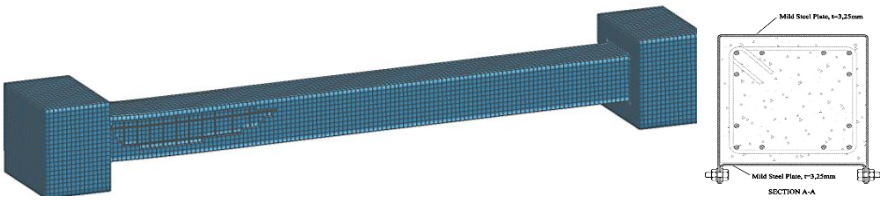

(b) Reinforced concrete column retrofitted by steel jacket 3.25mm

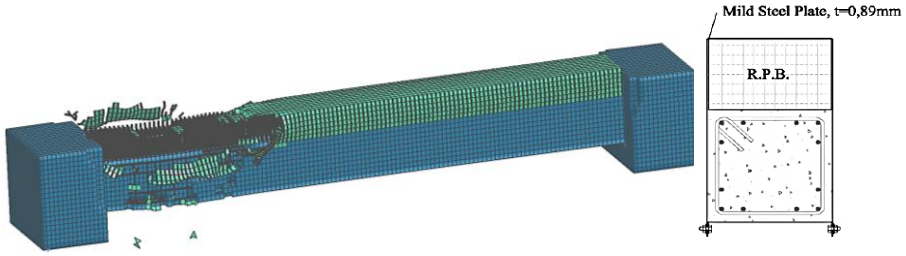

(c) Reinforced concrete column retrofitted by RPB with light steel jacket

Figure 15. Comparison of failure shapes under blast load for the different retrofitting systems

Table 10. Results of parametric study regarding maximum deflection values

Retrofit system	Variable	Deflection (mm)
No retrofit	f_{cu} 30 MPa	66.50
	f_{cu} 40 MPa	52.00
	f_{cu} 50 MPa	48.70
Steel jacket	Thickness 2mm	38.70
	Thickness 3.25mm	29.10
	Thickness 5mm	21.80
Reinforced Polyurethane Brick	Density 545.30 kg/m^3	55.60
	Density 569.30 kg/m^3	52.70
	Density 593.20 kg/m^3	51.65

Table 10 summarizes the results of the parametric study investigating the possible enhancement of the behavior of RC column under blast load effect. By comparing between the deflections value for three parametric studies, it is clear that the steel jacket protecting system is the best system in protecting the column and also to minimize the deflection value.

VI. Conclusion

This paper has presented numerical investigation of the response of RC elements under the effect of blast load and improvement of deflection and failure shape by two blast retrofitting alternatives. Three-dimensional finite element models are created and dynamic nonlinear analysis is made using the commercial program LS-DYNA. Numerical parametric study showed that the concrete compressive strength has a major effect on concrete splitting failure and deformed shape, the deflection is decreased by increasing the compressive strength.

Different sacrificial cladding system are used to work as protective systems such as steel jacket and reinforced polyurethane bricks with light jacketing (thickness=0.89mm). Numerical models are created for the two alternatives. The steel jacket protective system has a good efficiency on the dynamic response of RC member on blast loading; the failure shape is enhanced as per increase the steel jacket thickness, so the splitting of RC element is decrease according to the increase of the steel jacket thickness which effect on the protection of RC column by increase the strain ductility and the RC element toughness, the failure shape and deflection values clarify the effective of the steel jacket thickness.

Secondly, reinforced polyurethane bricks is the second alternative for protect the RC member to resist the blast loads, the deflection value is decreased slightly and also the failure shape. Accordingly, it is clear that the changing of densities and the stress-strain curve a slightly changing on the failure shape and deflection value.

Finally, as per previous numerical study using FE modeling by LS-DYNA software package on the different sacrificial cladding and changing the compressive strength of concrete, it is clear that the changing of compressive strength of concrete and steel jacket thickness have a large effect on the deformed shape, deflection value and concrete failure, as it enhanced all previous items and on the other side, it is clear that the reinforced polyurethane bricks has a lower influential than using steel jacket protection system.

References

[1]. Ibrahim, Y.E., Ismail, M.A. and Nabil, M. 2017. Response of reinforced concrete frame structures under blast loading, Procedia Engineering 171: 890–898.
[2]. Hallquist, O. 2012. LS-DYNA Keyword User's Manual, Volume II.
[3]. Kohnke, P. 2014. ANSYS theory reference release 5.6'. Canonsburg: SAS IP,Inc, p. Eleventh Edition.
[4]. Simulia 2014. ABAQUS Software, Dassault Systems, Simulia Corp.
[5]. Lange, D. 2013. A review of blast loading and explosions in the context of multifunctional buildings, Fire Technology SP Technical Research Institut of Sweden, Boras.
[6]. Zhou, X. and Hao, H. 2008. Prediction of airblast loads on structures behind a protective barrier. International Journal of Impact Engineering. 35: 363-375
[7]. Petropouleas, I., Croll, P. J., and Bassett, R. 2008. Vulnerability of reinforced concrete structural elements to internal explosions, RTO-MP-SET-125: 1–8. https://www.sto.nato.int/publications/STO%20Meeting%20Proceedings/RTO-MP-SET-125/MP-SET-125-52.pdf
[8]. Tan, S. H., Poon, J.K.Chan, R. and Chng, D. 2012. Retrofitting of reinforced concrete beam-column via steel jackets against close-in detonation, 12th International LS-DYNA Users Conference 3: 1–12.
[9]. Codina, R., Ambrosini, D. and de Borbón, F. 2016. Alternatives to prevent the failure of RC members under close-in blast loadings, Engineering Failure Analysis 60: 96–106.
[10]. Esmaeilnia Omran, M. and Mollaei, S. 2017. Investigation of axial strengthened reinforced concrete columns under lateral blast loading, Shock and Vibration, Article ID 3252543, 18 p.
[11]. Hanssen, A. G., Olovsson, L., Børvik, T. and Langseth, M. 2009. Close-range blast loading of aluminium foam panels: A numerical study, in IUTAM Bookseries, IUTAM Symposium on Mechanical Properties of Cellular Materials 12:169–180.
[12]. Codina, R., Ambrosini, D. and de Borbón, F. 2016. New sacrificial cladding system for the reduction of blast damage in reinforced concrete structures, Int. J. Protective Structures 8(2) 221–236.
[13]. Karlos, V., Solomos, G. and Larcher, M. 2016. Analysis of blast parameters in the near-field for spherical free-air explosions. EUR 27823, Publications Office of the European Union, Luxembourg.
[14]. Williams, G., Holland, C., Williamson, E. B., Bayrak O., Marchand K. A. and Ray, J. 2012. Blast-resistant highway bridges: design and detailing guidelines. WIT Transactions on State of the Art in Science and Engineering 60: 143-151.
[15]. Al-bayti, A. 2017. Vulnerability of reinforced concrete columns to external blast loading. Thesis. Ottawa, Canada.
[16]. Abladey L and Braimah A. 2014. Near-field explosion effects on the behaviour of reinforced concrete columns: A numerical investigation, Int. J. Protective Structures 5(4): 475–499.
[17]. Codina, R., Ambrosini, D. and de Borbón, F. 2016. Experimental and numerical study of a RC member under a close-in blast loading, Engineering Structures 127:145–158.
[18]. Leppänen, J. 2002. Dynamic behaviour of concrete structures subjected to blast and fragment impacts, Licentiate thesis, Chalmers University of Technology, Göteborg, Sweden.
[19]. Zakrisson, B., Wikman, B. and Häggblad, H. 2011. Numerical simulations of blast loads and structural deformation from near-field explosions in air, International Journal of Impact Engineering 38 (7): 597-612.
[20]. Bermejo, M., Jose M. Goicolea, J.M., Gabaldon, F. and Santos, A. 2011. Impact and explosive loads on concrete buildings using shell and beam type elements', ECCOMAS Thematic Conference - COMPDYN 2011: 3rd International Conference on Computational Methods in Structural Dynamics and Earthquake Engineering: An IACM Special Interest Conference, July 2011.
[21]. Thai, D. and Kim, S. 2018. Numerical investigation of the damage of RC members subjected to blast loading', Engineering Failure Analysis. Elsevier, 92(June), pp. 350–367.
[22]. Tai, Y.S., Chu, T., Hu, H-T. and Wu, J. 2011. Dynamic response of a reinforced concrete slab subjected to air blast. Theoretical and Applied Fracture Mechanics 56: 140-147.
[23]. Zidan, M. K., Fayed, M. N., Elhosiny, A. M., Abdelgawad, K. M. and Orfy, H. H. 2014. Modelling of damage patterns of RC concrete columns under demolition by blasting. WIT Transactions on the Built Environment 141: 95–111.
[24]. Koli, S. Chellapandi, P., Rao, L.B. and Swanti, A. 2020. Study on JWL equation of state for the numerical simulation of near-field and far-field effects in underwater explosion scenario, Engineering Science and Technology, an International Journal 23(4): 758–768.
[25]. Schwer, L. E. 1998. Conference Jones-Wilkens-Lee (JWL) equation of state with afterburning, 4th International LS-DYNA Users, Session: Constitutive Modeling, 1–38.
[26]. Belal, M. F., Mohamed, H. M. and Morad, S. A. 2015. Behavior of reinforced concrete columns strengthened by steel jacket, HBRC Journal. Housing and Building National Research Center 11(2): 201–212.
[27]. Elsanadedy, H. M. Almusallam, T.H., Alsayed, S.H., and Al-Salloum, Y.A. 2013. Flexural strengthening of RC beams using textile reinforced mortar – Experimental and numerical study. Composite Structures 97: 40–55.
[28]. Elsayed, A. K. 2014. Effect of longitudinal CFRP strengthening on the shear resistance of reinforced concrete beams, Composites: Part B 58: 422–429.
[29]. Lu, X. Z., Teng, J.G.,Ye, L.P. and J.Jiang, J.J. 2005. Bond-slip models for FRP sheets / plates bonded to concrete. Engineering Structures 27:920–937.
[30]. Lu, X. Z. Teng, J.G.,Ye, L.P. and J.Jiang 2007. Intermediate crack debonding in FRP-strengthened RC beams: FE analysis and strength model, Journal of Composites for Construction ASCE 11(2):161–174.
[31]. Mahmoud, M. M., Farag, H. M. and Mahfouz, S. Y. 2015. Behavior of reinforced concrete slab with aluminum foam panels subjected to blast loadings, International Conference on Aerospace Sciences and Aviation Technology ASAT-16, Military Technical College, Kobry Elkobbah, Cairo, Egypt, May 26 - 28, 2015.
[32]. Shah, Q. H. and Topa, A. 2014. Modeling large deformation and failure of expanded polystyrene crushable foam using LS-DYNA. Modelling and Simulation in Engineering, Article ID 292647.
[33]. Xia, Y., Wu, C., Zhang, F., Li, Z-X and Bennet, T. 2014. Numerical analysis of foam-protected RC members under blast loads, International Journal of Protective Structures 5(4):367–390.
[34]. Ashby, M. F. 1983. Mechanical properties of cellular solids, Metallurgical Transactions A: Physical Metallurgy and Materials Science 14 A(9):1755–1769.
[35]. Bornstein, H. and Ackland, K. 2013. Evaluation of energy absorbing materials under blast loading', WIT Transactions on Engineering Sciences, 77, pp. 125–136. 1.
[36]. Beals, J. T. and Thompson, M. S. 1997. Density gradient effects on aluminium foam compression behaviour, Journal of Materials Science 32(13): 3595–3600.

[37]. Wu, C., Oehlers, D. J. and Day, I. 2009. Layered blast capacity analysis of FRP retrofitted RC member, Advances in Structural Engineering 12(3): 435–449.
[38]. Jackson, K. E. 2010. Predicting the dynamic crushing response of a composite honeycomb energy absorber using solid-element-based, 11th International LS-DYNA Users Conference 2: 1–19.

Marco Fouad. et. al. "Numerical Investigation of Strengthening Alternatives for RC Members to Enhance Blast Resistance." *IOSR Journal of Mechanical and Civil Engineering (IOSR-JMCE)*, 18(4), 2021, pp. 19-32.